Available online at www.sciencedirect.com
ScienceDirect
Journal of Hazardous Materials 143 (2007) 362–371
Journal of Hazardous Materials
www.elsevier.com/locate/jhazmat

Continuous fixed bed biosorption of reactive dyes by dried *Rhizopus arrhizus*: Determination of column capacity

Zümriye Aksu *, Şeyda Şen Çağatay, Ferda Gönen

Hacettepe University, Chemical Engineering Department, 06532 Beytepe, Ankara, Turkey

Received 1 June 2006; received in revised form 22 August 2006; accepted 14 September 2006
Available online 19 September 2006

Abstract

A continuous fixed bed study was carried out by using dried *Rhizopus arrhizus* as a biosorbent for the removal of three reactive dyes; Gemacion (Procion) Red H-E7B (GR), a monoclorotriazine mono-azo type reactive dye; Gemazol Turquise Blue-G (GTB), a vinyl sulfone mono-azo type reactive dye and Gemactive (Reactive) Black HFGR (GB), a vinyl sulfone di-azo type reactive dye from aqueous solution. The effect of operating parameters such as flow rate and inlet dye concentration on the sorption characteristics of *R. arrhizus* was investigated at pH 2.0 and at 25 °C for each dye. Data confirmed that the total amount of sorbed dye decreased with increasing flow rate and increased with increasing inlet dye concentration for each dye. The column biosorption capacity of dried *R. arrhizus* was 1007.8 mg g^{-1} for GR dye, 823.8 mg g^{-1} for GTB dye and 635.7 mg g^{-1} for GB dye at the highest inlet dye concentration of approximately 750 mg l^{-1} and at the minimum flow rate of 0.8 ml min^{-1}. Thomas and Yoon–Nelson models were applied to experimental data to predict the breakthrough curves and to determine the biosorption capacity of the column for each dye useful for process design. Both models were found suitable for describing the whole dynamic behavior of the column with respect to flow rate and inlet dye concentration.

Keywords: *Rhizopus arrhizus*; Biosorption; Reactive dye; Fixed bed column; Breakthrough curve; Column capacity

1. Introduction

Because of their ease of use, inexpensive cost of synthesis, stability and variety of color compared with natural dyes, synthetic dyestuffs have been increasingly used in the textile, paper, rubber, plastics, cosmetics, pharmaceutical and food industries. Today there are more than 10,000 dyes available commercially, most of which are difficult to biodegrade due to their complex aromatic molecular structure and synthetic origin [1,2]. The extensive use of dyes often poses pollution problems in the form of colored wastewater discharge into environmental water bodies. Even small quantities of dyes can color large water bodies, which not only affects aesthetic merit but also reduces light penetration and photosynthesis. In addition, some dyes are either toxic or mutagenic and carcinogenic due to the presence of metals, chlorides, etc., in their structure [3–8].

There are many kinds of dyes available in the market. Based on the chromophore group, 20–30 different groups of dyes can be discerned. Anthraquinone, phthalocyanine, triarylmethane and azo dyes are quantitatively the most important groups. The azo dyes, characterized by having an azo group consisting of nitrogen nitrogen double bonds and the presence of bright color due to these azo bonds and associated chromophores, are the largest class of dyes used in textile industry. A wide variety of dyes, namely acid, reactive, disperse, vat, metal complex, mordant, direct, basic and sulphur dyes take place inside the azo dyes. Between these, the most used are the reactive azo dyes combined with different types of reactive groups. They differ from all other classes of dyes in that they bind to the textile fibres such as cotton to form covalent bonds. They have the favourable characteristics of bright color, water-fast, simple application techniques and low energy consumption and are used extensively in textile industries, but nearly 50% of reactive dyes may be lost to the effluent after dyeing of cellulose fibres. Reactive dyes cannot be easily removed by conventional wastewater treatment systems since they are stable to light, heat and oxidizing agents and are biologically non-degradable so they have therefore been identified as problematic compounds in textile effluents. Hence their removal is also of great importance [1,2,8].

* Corresponding author. Tel.: +90 312 2977434; fax: +90 312 2992124.
E-mail address: zaksu@hacettepe.edu.tr (Z. Aksu).

0304-3894/$ – see front matter © 2006 Elsevier B.V. All rights reserved.
doi:10.1016/j.jhazmat.2006.09.039

Nomenclature

C	effluent dye concentration (mg l^{-1})
C_0	inlet (feed) dye concentration (mg l^{-1})
C_{ad} (=$C_0 - C$)	adsorbed dye concentration in the column (mg l^{-1})
k_{Th}	kinetic constant in Thomas model (ml mg^{-1} min^{-1})
k_{YN}	kinetic constant in the Yoon and Nelson model ($l\,min^{-1}$)
m_{total}	total amount of dye fed to column (mg)
q_{eq}	equilibrium dye uptake per gram of biosorbent in the column (column capacity) (mg g^{-1})
q_{total}	total adsorbed quantity of dye in the column (mg)
q_0 (=q_{eq})	constant in Thomas model indicated the column capacity (mg g^{-1})
Q	flow rate (ml min^{-1})
t	flow time (min)
t_{break}	time at breakthrough (min)
t_{total}	total flow time (min)
V_{eff}	effluent volume (ml)
X	amount of sorbent in the column (g)

Greek letter

τ	time required for 50% adsorbate breakthrough (min)

Although some existing technologies – conventional chemical coagulation/flocculation, ozonation, oxidation, adsorption – may have a certain efficiency in the removal of reactive dyes, their initial and operational costs are so great that they constitute an inhibition to dyeing and finishing industries [3–7]. This has led many workers to search for the use of cheap, efficient and easily available alternative materials of agricultural and biological origin, along with industrial by-products, as adsorbents. Using microorganisms such as bacteria, fungi, yeast and algae as biosorbents for textile dyes also offers a potential alternative to existing methods for detoxification. The uptake of chemicals from aqueous solution by microbial mass by physicochemical mechanisms has been termed as biosorption. This term is used to indicate a number of metabolism-independent processes (physical and chemical adsorption, ion exchange, complexation, chelation and microprecipitation) taking place essentially in the cell wall. The mechanism of binding by inactivated biomass may depend on the chemical nature of pollutant (species, size, ionic charge), type of biomass, its preparation and its specific surface properties and environmental conditions (pH, temperature, ionic strength, existence of competing organic or inorganic ligands in solution). As hydrophobic organic pollutants show a high tendency to accumulate onto microbial cells or sludge, the microbial biomass could be used as an adsorbent of biological origin for the removal of very low concentration hazardous organics from the wastewater [7–18].

Numerous studies on biosorption of heavy metals and organics in batch systems have been reported in the literature. However, in practice the column type continuous flow operations which are more useful in large-scale wastewater treatment have distinct advantages over batch treatment. It is simple to operate, attains a high yield and it can be easily scaled up from a laboratory-scale procedure. The stages in the separation protocol can also be automated and high degrees of purification can often be achieved in a single step process. A packed bed is also an effective process for cyclic sorption/desorption, as it makes the best use of the concentration difference known to be a driving force for adsorption and allows more efficient utilization of the sorbent capacity and results in a better quality of the effluent. A large volume of wastewater can be continuously treated using a defined quantity of sorbent in the column. Reuse of microorganism is also possible. After pollutant loading the pollutant may be concentrated in a small volume of solid material or desorbed into a small volume of eluant for recovery, disposal or containment [19–30].

The ability of *Rhizopus arrhizus* biomass to remove and accumulate heavy metals and organics has been recognized and studied to a certain degree for its biosorption capability [8]. However there has been limited research on the biosorption of textile dyes by the biomass to date [12,15,28]. Moreover very few papers have reported the dye adsorption by *R. arrhizus* at continuous flow conditions [28]. In this study, a process of biosorption of Gemacion (Procion) Red H-E7B, Gemazol Turquise Blue-G and Gemactive (Reactive) Black HFGR dyes onto dried *R. arrhizus* was investigated in a continuous fixed bed as a function of flow rate and inlet dye concentration. These dyes were chosen because of their widespread use as reactive azo dyes for dying cellulose fibers in Turkish textile industry with relatively high consumption rate and being quite common pollutants in wastewasters from the textile industry. Thomas and Yoon–Nelson models were applied to experimental data to simulate the breakthrough curves and to find the column capacity in order to predict the scale-up of a unit plant.

2. Mathematical description of biosorption in a continuous fixed bed

The performance of packed bed is described through the concept of the breakthrough curve. Both, the time until the sorbed species are detected in the column effluent (breakthrough point) at a given concentration, and the shape of the concentration–time profile or breakthrough curve, are very important characteristics for operation, dynamic response and process design of a biosorption column because they directly affect the feasibility and economics of the sorption phenomena. Experimental determination of these parameters is very dependent on column operating conditions such as feed pollutant concentration and flow rate. A breakthrough curve is usually expressed in terms of adsorbed pollutant concentration (C_{ad} = ⟨net pollutant concentration (C_0) − outlet pollutant concentration (C)⟩) or normalized concentration defined as the ratio of effluent pollutant concentration to inlet pollutant concentration (C/C_0) as a function of flow time (t) or volume of effluent (V_{eff}) for a given bed height.

Effluent volume (V_{eff}) calculated from Eq. (1):

$$V_{eff} = Qt_{total} \quad (1)$$

where t_{total} and Q are the total flow time and volumetric flow rate.

The area under the breakthrough curve (A) can be obtained by integrating the adsorbed concentration (C_{ad}) versus t plot. Total adsorbed pollutant quantity (q_{total}) in the column for a given feed concentration and flow rate is calculated from Eq. (2):

$$q_{total} = \frac{QA}{1000} = \frac{Q}{1000}\int_{t=0}^{t=t_{total}} c_{ad}\,dt \quad (2)$$

Total amount of pollutant sent to column (m_{total}) is calculated from Eq. (3):

$$m_{total} = \frac{C_0 Qt_{total}}{1000} \quad (3)$$

Total removal percent of pollutant (column performance) with respect to flow volume can be also found from the ratio of total adsorbed quantity of pollutant (q_{total}) to the total amount of pollutant sent to column (m_{total}) (Eq. (4)):

$$\text{total removal } \% = \frac{q_{total}}{m_{total}} \times 100 \quad (4)$$

Equilibrium dye uptake (q_{eq}) (or column capacity) in the column is defined by Eq. (5) as the total amount of dye sorbed (q_{total}) per gram of sorbent (X) at the end of total flow time:

$$q_{eq} = \frac{q_{total}}{X} \quad (5)$$

Successful design of a column adsorption process requires prediction of the concentration-time profile or breakthrough curve and adsorption capacity for the effluent under given specific operating conditions. Developing a model to accurately describe the dynamic behavior of adsorption in a fixed bed system is inherently difficult as in such systems the concentration profiles in the liquid and adsorbent phases vary in both space and time. Some solutions for very limiting cases have been reported, but in general, complete time-dependent analytical solutions to differential equation based models of the proposed rate mechanisms are not available. If the goal is to model the breakthrough behavior of a biosorption column with a high degree of accuracy, the use of simpler and more tractable models that avoid the need for numerical solution appears more suitable and logical and could have immediate practical benefits. Several such models have been applied to biosorption columns [2,22–32] and the following Thomas [31] and Yoon–Nelson [32] models used in the literature to characterize the fixed bed performance for the removal of dyes are presented here. Besides the prediction of the concentration-time profile or breakthrough curve for the effluent, the models also give an idea about the adsorption capacity of adsorbent. The linearized form of the Thomas model is as follows:

$$\ln\left(\frac{C_0}{C} - 1\right) = \frac{k_{Th}q_{0Th}X}{Q} - \frac{k_{Th}C_0}{Q}V_{eff} \quad (6)$$

where k_{Th} is the Thomas rate constant, q_{0Th} the maximum solid-phase concentration of the solute (column capacity), Q the flow rate and X is the amount of sorbent in the column. The kinetic coefficient k_{Th} and the adsorption capacity of the bed q_{0Th} can be determined from a plot of $\ln((C_0/C) - 1)$ against V_{eff} at a given flow rate.

Yoon and Nelson have developed a relatively simple model addressing the adsorption and breakthrough of adsorbate vapors or gases with respect to activated charcoal. This model is based on the assumption that the rate of decrease in the probability of adsorption for each adsorbate molecule is proportional to the probability of adsorbate adsorption and the probability of adsorbate breakthrough on the adsorbent. The Yoon and Nelson model not only is less complicated than other models, but also requires no detailed data concerning the characteristics of adsorbate, the type of adsorbent, and the physical properties of adsorption bed [32]. The linear form of Yoon and Nelson equation regarding to a single-component system is expressed as

$$\ln\left(\frac{C}{C_0 - C}\right) = k_{YN}t - \tau k_{YN} \quad (7)$$

where k_{YN} is the Yoon–Nelson rate constant; τ the time required for 50% adsorbate breakthrough and t is the breakthrough (sampling) time. The parameters k_{YN} and τ may be determined from a plot of $\ln(C/(C_0 - C))$ versus sampling time (t). The derivation of Eq. (7) was based on the definition that 50% breakthrough occurs at $t = \tau$. Thus, the adsorption bed should be completely saturated at $t = 2\tau$. Owing to the symmetrical nature of breakthrough curves due to the Yoon–Nelson model, the amount of dye being adsorbed in the fixed bed is half of the total dye entering the adsorption bed within 2τ period. Hence, the following equation can be obtained for a given bed:

$$q_{0YN} = \frac{q_{total}}{X} = \frac{(1/2)C_0(Q/1000)(2\tau)}{X} = \frac{C_0 Q\tau}{1000X} \quad (8)$$

This equation also permits one to determine the adsorption capacity of the column (q_{0YN}) as a function of inlet dye concentration (C_0), flow rate (Q), biomass quantity in the column (X) and 50% breakthrough time (τ) by using the Yoon–Nelson model [25] and [27].

3. Experimental

3.1. Microorganism and growth conditions

R. arrhizus, a filementous fungus obtained from the US Department of Agriculture Culture Collection was used in this study. The microorganism was grown at 25 °C in agitated liquid media containing malt extract (17 g l^{-1}) and soya peptone (5.4 g l^{-1}). The pH of the medium was adjusted to 6.5–6.8 with dilute H_2SO_4 and NaOH solutions before sterilization.

3.2. Preparation of the microorganism and dye solutions for biosorption

After the growth period *R. arrhizus* was washed twice with distilled water, inactivated using 1% formaldehyde for 1 h and then washed again with distilled water and dried at 60 °C for 24 h. Dried biomass grounded and sieved to 210–300 μm and

filled into the column. Then, the bed was rinsed with distilled water and left overnight to ensure a closely packed arrangement of particles without voids, channels, or cracks.

Gemacion (Procion) Red H-E7B (C.I. Reactive Red 141; empirical formula $C_{52}H_{34}O_{26}S_8Cl_2N_{14}$; molecular weight = 1774), a commercial homo-bireactive mono-azo dye composed of two monochlorotriazine reactive groups; Gemazol Turquoise Blue G (C.I. Reactive Blue 21; empirical formula $CuPc(SO_3H)_{2-3}(C_8H_8O_4S_2N)_{1-2}$; molecular weight = 576.1), a commercial mono-azo dye containing vinyl sulfone as reactive group and copper phthalocyanine as chromophore group and Gemactive (Reactive) Black (C.I. RB5 or (Remazol Black B; empirical formula $C_{26}H_{21}O_{19}N_5S_6Na_4$; molecular weight = 991.8), a commercial di-azo dye containing vinyl sulfone as reactive group, were kindly supplied by Gemsan, Turkey and used as received without further purification. The test solutions containing required dye were prepared by diluting 1.0 g l^{-1} of stock solution of each dye which was obtained by dissolving weighed quantity of dye in 1 l of double-distilled water. The range of concentrations of prepared dye solutions changed between 100 and 800 mg l^{-1}. The pH of each feed solution was adjusted to 2.0 with diluted or concentrated H_2SO_4 solutions before contacting the biomass.

3.3. Sorption studies in the continuous system

Continuous packed bed studies were performed in a fixed bed mini glass column with an inside diameter of 0.96 cm, a bed depth of 6.0 cm and 1.63 g of dried cells. For each dye, the dye solution at a known concentration and flow rate was passed continuously through the stationary bed of sorbent in up-flow mode to avoid channelling of the effluent. The flow rate was regulated with a variable speed peristaltic pump by Masterflex CL (Model 77120-60). Samples of the effluent were collected periodically and analysed for the remaining dye concentration as described below. The experiment was continued until a constant concentration of dye was obtained. The column studies were performed at the optimum pH value of 2.0 determined from the previous batch system studies, and at a constant temperature of 25 °C to be representative of environmentally relevant conditions.

All the experiments were carried out in duplicates and the average values were used for further calculations.

3.4. Analysis of dyes

The concentration of unadsorbed Gemazol Turquise Blue-G, Gemacion Red H-E7B and Gemactive Black HFGR dyes in the biosorption media were measured colorimetrically using a spectrophotometer (Bausch and Lomb-Spectronic 20D, Milton Roy Company, USA). The absorbance of the color of Gemazol Turquise Blue-G, Gemacion Red H-E7B and Gemactive Black HFGR was read at 341, 544 and 595 nm, respectively.

4. Results and discussion

The biosorption of Gemacion Red H-E7B, Gemazol Turquise Blue-G and Gemactive Black HFGR three different structured reactive dyes to dried *R. arrhizus* was investigated in a continuous fixed bed column as a function of flow rate and inlet dye concentration. The results are given as units of ratio of effluent dye concentration to inlet dye concentration (normalized dye concentration) (C/C_0), total amount of dye sorbed (q_{total}; mg) equilibrium uptake (or column capacity) (q_{eq}; mg g^{-1}) and total removal percent of dye (column performance).

The preliminary studies showed that the uptake of each dye was affected seriously by the change of pH of biosorption medium. Upon dissolution, ionic dyes release colored dye anions into solution. The adsorption of these charged dye groups onto the adsorbent surface is primarily influenced by the surface charge that in turn is influenced by the solution pH. With diminishing pH increasing numbers of weak base groups in the biomass become protonated and gain a net positive charge. These charged sites become available for binding anionic groups such as the reactive dyes used in this study at lower pH values [28]. So the working pH value for each dye was chosen as 2.0 as the highest uptake of each dye was obtained at this pH value.

4.1. Effect of flow rate

The effect of flow rate on the Gemacion Red H-E7B, Gemazol Turquise Blue-G and Gemactive Black HFGR dyes sorption characteristics of dried *R. arrhizus* in the continuous-flow fixed bed column was examined by varying the flow rate from 0.8 to 3.2 ml min^{-1} while the bed height and inlet dye concentration was held constant at 6.0 cm and at 100 mg l^{-1}, respectively. The plots of comparative normalized dye concentration (C/C_0) versus effluent volume at different flow rates (symbols) are shown in Figs. 1–3 for each dye together with the breakthrough curves (lines) calculated from Eqs. (6) and (7) which are discussed later. The results show that the adsorption of each dye onto the biomass surface was strongly dependent on flow rate. From the figures, initially, each dye was rapidly adsorbed on the biomass due to the availability of reaction sites able to capture the dye ions around or inside the cells, and the effluent (from the upper part of the bed) was almost free of solute. As the dye solution

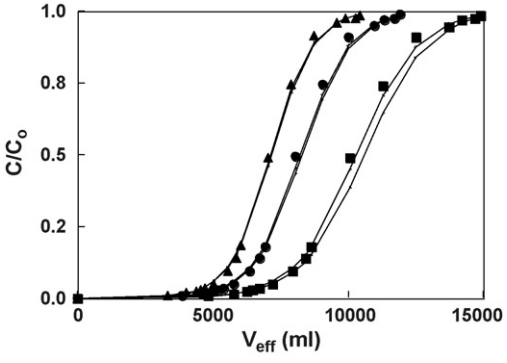

Fig. 1. Comparison of the experimental and predicted breakthrough curves of Gemacion Red H-E7B(A) dye biosorption obtained at different flow rates (C_0: 100 mg l^{-1}; T: 25 °C, initial pH: 2.0). (■) Q: 0.8 ml min^{-1}; exp, Q: 0.8 ml min^{-1}; Thomas, Q: 0.8 ml min^{-1}; Yoon–Nelson. (●) Q: 1.6 ml min^{-1}; exp, Q: 1.6 ml min^{-1}; Thomas, Q: 1.6 ml min^{-1}; Yoon–Nelson (▲) Q: 3.2 ml min^{-1}; exp, Q: 3.2 ml min^{-1}; Thomas, Q: 3.2 ml min^{-1}; Yoon–Nelson.

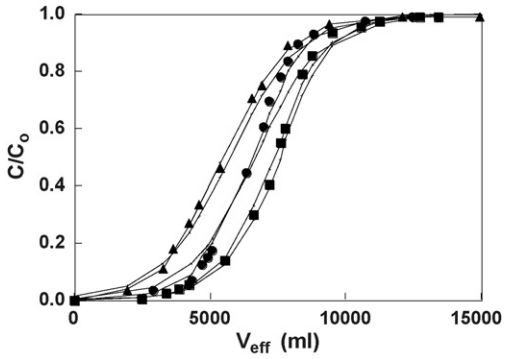

Fig. 2. Comparison of the experimental and predicted breakthrough curves of Gemazol Turquise Blue-G dye biosorption obtained at different flow rates (C_0: 100 mg l^{-1}; T: 25 °C, initial pH: 2.0). (■) Q: 0.8 ml min^{-1}; exp, Q: 0.8 ml min^{-1}; Thomas, Q: 0.8 ml min^{-1}; Yoon–Nelson. (●) Q: 1.6 ml min^{-1}; exp, Q: 1.6 ml min^{-1}; Thomas, Q: 1.6 ml min^{-1}; Yoon–Nelson (▲) Q: 3.2 ml min^{-1}; exp, Q: 3.2 ml min^{-1}; Thomas, Q: 3.2 ml min^{-1}; Yoon–Nelson.

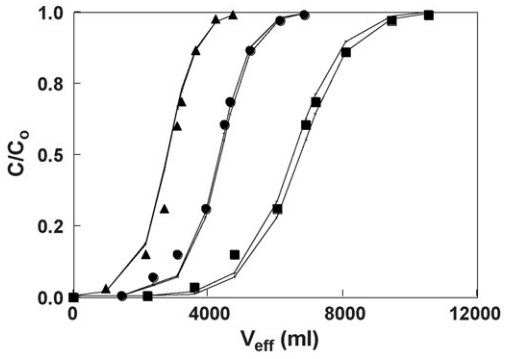

Fig. 3. Comparison of the experimental and predicted breakthrough curves of Gemactive Black HFGR dye biosorption obtained at different flow rates (C_0: 100 mg l^{-1}; T: 25 °C, initial pH: 2.0). (■) Q: 0.8 ml min^{-1}; exp, Q: 0.8 ml min^{-1}; Thomas, Q: 0.8 ml min^{-1}; Yoon–Nelson. (●) Q: 1.6 ml min^{-1}; exp, Q: 1.6 ml min^{-1}; Thomas, Q: 1.6 ml min^{-1}; Yoon–Nelson (▲) Q: 3.2 ml min^{-1}; exp, Q: 3.2 ml min^{-1}; Thomas, Q: 3.2 ml min^{-1}; Yoon–Nelson.

continued to flow, due to the gradual occupancy of these sites, the uptake became less effective and, therefore, the outlet concentration started to increase until the saturation point was reached. All the breakthrough curves of dyes followed the typical S-shape curve for column operation. The breakthrough curves became steeper and shifted to the origin with increasing flow rate while the breakpoint time decreased. The use of high flow rates reduces the time that dye in the solution is in contact with the biomass, thus allowing less time for biosorption to occur, leading to an early breakthrough of dye. The column sorption data of each dye were evaluated and the total sorbed quantities, equilibrium dye uptakes and removal percents with respect to flow rate are presented in Table 1. In general increasing flow rate resulted in a decrease of all these values.

The plots of dimensionless concentration (C/C_0) of Gemacion Red H-E7B dye versus time at different flow rates are shown in Fig. 1. An earlier breakthrough and exhaustion time were observed in the profile when the flow rate increased from 0.8 to 3.2 ml min^{-1} resulting in lower uptake and lower percent removal. As shown in Fig. 1, the breakthrough ($C/C_0 = 0.05$) occurs at 150.0, 60.0 and 26.4 h for flow rate of 0.8, 1.6 and 3.2 ml min^{-1}, respectively. As seen in Table 1, the flow rate also strongly influenced the Gemacion Red H-E7B uptake capacity of dried biomass as 615.6, 471.8 and 460.4 mg g^{-1}, which were recorded at 0.8, 1.6 and 3.2 ml min^{-1}, respectively. This behavior may be due to insufficient time for the solute inside the column and the diffusion limitations of the solute into the pores of the sorbent at higher flow rates.

For the biosorption of Gemazol Turquise Blue-G when the flow rate increased from 0.8 to 3.2 ml min^{-1} the time required for breakthrough decreased from 88.0 h to about 12.6 h. Increasing flow rate from 0.8 to 3.2 ml min^{-1} also reduced the volume of water treated from 4224 to 2400 ml for the dye treatment (Fig. 2). Corresponding decrease in sorption capacity from 430.4 to 332.9 mg g^{-1} was observed when flow rate raised from 0.8 to 3.2 ml min^{-1} (Table 1). This decrease in breakthrough time can be due to relatively low contact time between solute and sorbent which further results in low diffusion of solute into the pores of the sorbent.

The breakthrough curves of Gemactive Black HFGR dye developed at three different flow rates (0.8, 1.6 and 3.2 ml min^{-1}) are presented in Fig. 3 for the inlet dye concentration of 100 mg l^{-1}. As said before for the two dyes, the time required to reach breakthrough also decreased for this dye as the flow

Table 1
Effect of flow rate on the total amount of dye sent to column (m_{total}), total adsorbed quantity of dye (q_{total}), equilibrium dye uptake (column capacity) (q_{eq}) and total removal percentage of dye

C_0 (mg l^{-1})	Q (ml min^{-1})	m_{total} (mg)	q_{total} (mg)	q_{eq} (mg g^{-1})	Dye removal %
Gemacion red H-E7B(A)					
99.0	0.8	1527.2	1003.4	615.6	65.7
101.3	1.6	1506.3	769.0	471.8	59.0
103.1	3.2	1471.4	750.4	460.4	51.0
Gemazol turquise Blue-G					
98.0	0.8	1246.1	701.6	430.4	56.3
95.9	1.6	1197.2	624.9	383.4	52.2
96.3	3.2	1164.4	542.6	332.9	46.6
Gemactive black HFGR					
99.6	0.8	1181.8	657.1	403.1	55.6
102.2	1.6	911.7	434.9	266.8	47.7
98.6	3.2	624.8	284.3	174.4	45.5

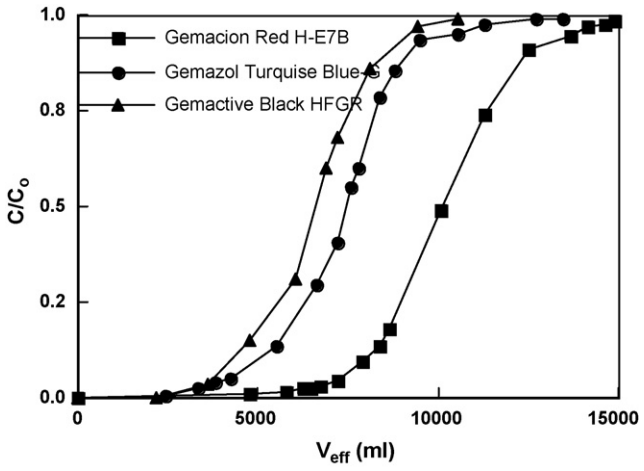

Fig. 4. Comparison of the experimental breakthrough curves of Gemacion Red H-E7B(A), Gemazol Turquise Blue-G and Gemactive Black HFGR dyes obtained at 0.8 ml min^{-1} flow rate and at an initial dye concentration of 100 mg l^{-1} (T: 25 °C, initial pH: 2.0).

rate increased. As a result, the bed utilization as well as the bed adsorption capacity was reduced. The volume of dye solution treated was the highest at the minimum flow rate of 0.8 ml min^{-1} and this flow rate displayed a relatively high dye removal and maximum values of total sorbed dye quantity, dye uptake and dye removal percentage were determined as 657.1 mg, 403.1 mg g^{-1} and 55.6%, respectively, at this flow rate.

In general, for all the dye ions, the breakthrough curves became steeper and the breakthrough time decreased with increasing flow rate. The higher adsorption yields obtained at lower flow rates (Table 1) can be explained by the fact that at higher flow rates the residence time of the solute in the column is too short and the solute does not have enough time to interact with the surface sorbent and diffuse into the pores. Even though more shortened mass transfer zone (usually preferable) was observed at the highest flow rate, the total dye removal percentage which is a reflective of system performance and the dye uptake were actually observed maximum at the lowest flow rate. The increase in sorption capacity with increasing residence time (low flow rates) indicates that the sorption process is controlled by intraparticle mass transfer. If the sorption process is intraparticle mass transfer controlled, a slower flow rate will provide a longer residence time for sorption to take place and the bed capacity will be higher.

Although dried *R. arrhizus* has a high potential as a biosorbent for the adsorption of all reactive dyes studied, it could be concluded from the shapes of breakthrough curves given in Fig. 4 that, the affinity of Gemacion Red H-E7B dye towards the dried *R. arrhizus* biomass is much more higher than that of Gemazol Turquise Blue-G and Gemactive Black HFGR dyes. Compared to the highest Gemazol Turquise Blue-G and Gemactive Black HFGR dyes uptakes (823.8 mg g^{-1} for GTB dye and 635.7 mg g^{-1} for GB dye), Gemacion Red H-E7B was removed more effectively by the biomass with an uptake capacity of 1007.8 mg g^{-1}. In the present work three representative reactive dyestuffs with different reactive (vinylsulphone, monochlorotriazine) and chromophore (mono-azo, di-azo, phythalocyanine) groups were studied so each dye molecule have amino, sulphonic and hydroxyl groups as substituents bound to the aromatic rings. Those functional groups could interact with the active groups on fungal biomass surface such as chitin, acidic polysaccharides, lipids, amino acids and other cellular components of the microorganism. The adsorption mechanism could be based on multiple interactions such as electrostatic, hydrophobic, van der Waals and hydrogen bonds due to pH. The variation in the sorption capacity between the dyes could be related to the molecular structure of dye, type and concentration of reactive groups and number of free electrons of the dye molecule resulting from several aromatic rings and double bonds responsible for the interaction with the biomass [7,12,28].

4.2. Effect of inlet dye concentration

The column biosorption performance of dried *R. arrhizus* for Gemacion Red H-E7B(A), Gemazol Turquise Blue-G and Gemactive Black HFGR dyes was also tested at various inlet dye concentrations. The sorption breakthrough curves obtained by changing inlet dye concentration from approximately 100 to 750 mg l^{-1} at 0.8 ml min^{-1} flow rate are given in Figs. 5–7 for each dye. Basically, the curves have the same and relatively sharp shape for all dyes (more shortened mass transfer zone) indicating that the axial dispersion is insignificant at higher dye concentrations. As expected, a decreased inlet dye concentration gave a later breakthrough curve and the treated volume was the greatest at the lowest inlet dye concentration since the lower concentration gradient caused a slower transport. The equilibrium dye uptakes, total sorbed dye quantities and dye removal percentages related to the inlet dye concentration are also compared in Table 2. For three dyes the amount of total sorbed dye, equilibrium dye uptake and total removal percent increased with increasing inlet dye concentration. A high concentration difference between the dye on the biosorbent and the dye in the solution provides the high driving force for the adsorption process and this may explain why higher adsorption

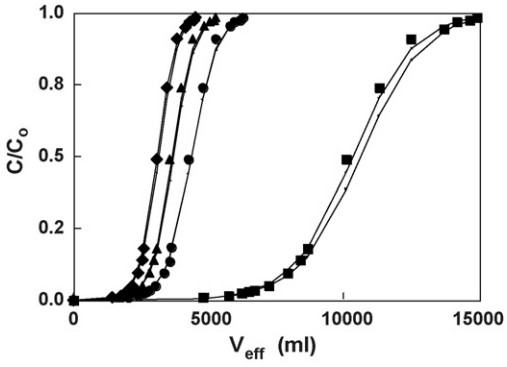

Fig. 5. Comparison of the experimental and predicted breakthrough curves of Gemacion Red H-E7B(A) biosorption obtained at different inlet dye concentrations (Q: 0.8 ml min^{-1}; T: 25 °C, initial pH: 2.0). (■) C_0: 100 mg l^{-1}; exp, C_0: 100 mg l^{-1}; Thomas, C_0: 100 mg l^{-1}; Yoon–Nelson. (●) C_0: 250 mg l^{-1}; exp, C_0: 250 mg;l^{-1}; Thomas, C_0: 250 mg l^{-1}; Yoon–Nelson. (▲) C_0: 500 mg l^{-1}; exp, C_0: 500 mg l^{-1}; Thomas, C_0: 500 mg l^{-1}; Yoon–Nelson. (♦) C_0: 750 mg l^{-1}; exp, C_0: 750 mg l^{-1}; Thomas, C_0: 750 mg l^{-1}; Yoon–Nelson.

Table 2
Effect of inlet dye concentration on the total amount of dye sent to column (m_{total}), total adsorbed quantity of dye (q_{total}), equilibrium dye uptake (column capacity) (q_{eq}) and total removal percentage of dye

C_0 (mg l^{-1})	m_{total} (mg)	q_{total} (mg)	q_{eq} (mg g^{-1})	Dye removal %
Gemacion Red H-E7B(A)				
99.8	1527.2	1003.4	615.6	65.7
251.6	1617.4	1085.3	665.8	67.1
503.4	2019.0	1383.0	848.5	68.5
751.3	2377.3	1642.7	1007.8	69.1
Gemazol Turquise Blue-G				
98.0	1246.1	701.6	430.4	56.3
254.1	1570.0	909.1	557.7	57.9
482.1	1967.9	1163.0	713.5	59.1
776.3	2238.0	1342.8	823.8	60.0
Gemactive Black HFGR				
103.2	1181.8	657.1	403.1	55.6
252.4	1314.5	751.9	461.3	57.2
501.6	1431.9	917.9	563.1	64.1
754.7	1541.9	1036.2	635.7	67.2

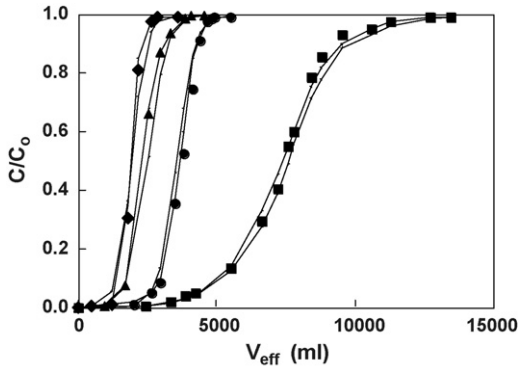

Fig. 6. Comparison of the experimental and predicted breakthrough curves of Gemazol Turquise Blue-G biosorption obtained at different inlet dye concentrations (Q: 0.8 ml min^{-1}; T: 25 °C, initial pH: 2.0). (■) C_0: 100 mg l^{-1}; exp, C_0: 100 mg l^{-1}; Thomas, C_0: 100 mg l^{-1}; Yoon–Nelson. (●) C_0: 250 mg l^{-1}; exp, C_0: 250 mg;l^{-1}; Thomas, C_0: 250 mg l^{-1}; Yoon–Nelson. (▲) C_0: 500 mg l^{-1}; exp, C_0: 500 mg l^{-1}; Thomas, C_0: 500 mg l^{-1}; Yoon–Nelson. (♦) C_0: 750 mg l^{-1}; exp, C_0: 750 mg l^{-1}; Thomas, C_0: 750 mg l^{-1}; Yoon–Nelson.

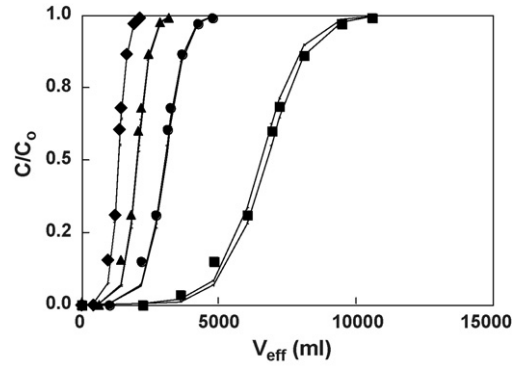

Fig. 7. Comparison of the experimental and predicted breakthrough curves of Gemactive Black HFGR biosorption obtained at different inlet dye concentrations (Q: 0.8 ml min^{-1}; T: 25 °C, initial pH: 2.0). (■) C_0: 100 mg l^{-1}; exp, C_0: 100 mg l^{-1}; Thomas, C_0: 100 mg l^{-1}; Yoon–Nelson. (●) C_0: 250 mg l^{-1}; exp, C_0: 250 mg l^{-1}; Thomas, C_0: 250 mg l^{-1}; Yoon–Nelson. (▲) C_0: 500 mg l^{-1}; exp, C_0: 500 mg l^{-1}; Thomas, C_0: 500 mg l^{-1}; Yoon–Nelson. (♦) C_0: 750 mg l^{-1}; exp, C_0: 750 mg l^{-1}; Thomas, C_0: 750 mg l^{-1}; Yoon–Nelson.

capacities were achieved in the column fed with a higher dye concentration than that with a lower dye concentration for each case.

The breakthrough curves obtained by changing Gemacion Red H-E7B(A) concentration from 100 to 750 mg l^{-1} at 0.8 ml min^{-1} flow rate are shown in Fig. 5. A decreased inlet Gemacion Red H-E7B(A) concentration gave an extended breakthrough curve and the treated volume was also higher, since the lower concentration gradient caused a slower transport due to decreased diffusion coefficient and decreased mass transfer coefficient. Binding sites are quickly filled at higher initial dye concentration resulting a decrease in breakthrough time. More favorable and steep breakthrough curves were obtained for higher Gemacion Red H-E7B(A) dye concentrations. From Table 2, it was observed that the highest uptake and highest percent removal of Gemacion Red H-E7B(A) (69.1%) were obtained for the highest dye concentration. Thus high driving force due to high dye concentration resulted in a better column performance.

The sorption breakthrough curves for Gemazol Turquise Blue-G obtained at different initial sorbate concentrations are shown in Fig. 6. Much sharper breakthrough curves, an indicator of shortened mass transfer zone which is usually preferable, were obtained especially at higher inlet dye concentrations. As expected, the breakpoint time for a higher dye concentration was earlier than that for a lower influent dye concentration as the binding sites became more quickly saturated in the system at higher dye concentrations. Table 2 shows that for the inlet dye concentrations of 98.0 and 776.3 mg l^{-1}, 56.3 and 60.0% of total dye applied to the column was adsorbed by dried *R. arrhizus* cells, respectively. The equilibrium dye uptake increased from 430.4 to 823.8 mg g^{-1} for the biomass with an increase of inlet dye concentration from 98.0 to 776.3 mg l^{-1}.

The biosorption performance of Gemactive Black HFGR was also tested at various inlet dye concentrations varying from 103.2 to 754.7 mg l^{-1}. An increase in the inlet dye concentration significantly affected the breakthrough curve as illustrated

Table 3
Parameters predicted from the Thomas and Yoon–Nelson models and model deviations obtained by linear and non-linear regression analysis for Gemazol Turquise Blue-G, Gemacion Red H-E7B(A) and Gemactive Black HFGR biosorptions onto dried *R. arrhizus* at different inlet dye concentrations and flow rates

C_0 (mg l^{-1})	Q (ml min^{-1})	$q_{eq,exp}$ (mg g^{-1})	k_{Th} ($\times 10^3$ ml mg^{-1} min^{-1})	q_{0Th} (mg g^{-1})	R^2	k_{YN} ($\times 10^3$ l min^{-1})	τ (min)	q_{0YN} (mg g^{-1})	R^2
Gemacion Red H-E7B(A)									
99.8	0.8	615.6	7.56	632.9	0.996	0.70	13266.3	621.4	0.994
251.6	0.8	665.8	6.87	670.0	0.997	1.71	5461.2	656.2	0.997
503.4	0.8	848.5	5.35	853.6	0.996	2.73	3444.2	837.1	0.990
751.3	0.8	1007.8	4.49	1015.7	0.994	3.42	2733.4	995.3	0.989
103.1	1.6	471.8	19.77	463.7	0.997	1.80	5189.7	455.6	0.991
101.2	3.2	460.4	42.00	438.5	0.995	4.20	2233.5	432.5	0.990
Gemazol Turquise Blue-G									
98.0	0.8	430.4	7.48	437.7	0.988	0.70	9833.3	447.9	0.979
254.1	0.8	557.7	10.57	562.8	0.963	2.40	4434.0	583.8	0.973
482.1	0.8	713.5	6.47	746.0	0.991	2.50	3154.1	689.8	0.976
776.3	0.8	823.8	4.65	891.0	0.969	3.11	2395.0	915.5	0.951
95.9	1.6	383.4	1.50	388.5	0.966	1.31	4181.5	386.3	0.947
96.3	3.2	332.9	2.63	334.7	0.986	2.52	1794.9	329.9	0.986
Gemactive Black HFGR									
103.2	0.8	403.1	10.66	414.7	0.980	1.10	8189.6	399.2	0.978
252.4	0.8	461.3	9.35	464.9	0.979	2.30	3851.4	454.1	0.974
501.6	0.8	563.1	7.06	623.2	0.977	3.51	2562.0	559.2	0.967
754.7	0.8	635.7	6.93	621.7	0.980	5.21	1688.1	608.4	0.980
99.9	1.6	266.8	32.62	270.0	0.978	3.30	2716.9	243.4	0.970
101.4	3.2	174.4	74.11	167.5	0.975	7.20	877.7	182.6	0.975

in Fig. 7. Inverse relationship between initial dye concentration and throughput volume was also observed for this dye. Higher inlet dye concentrations caused a faster breakthrough as expected. When the inlet dye concentration increased from 103.2 to 754.7 mg l^{-1}, the corresponding adsorption bed capacity increased from 403.1 to 635.7 mg g^{-1}. Table 3 also shows that highest uptake and dye removal were obtained at the highest dye concentration.

These results demonstrated that the change of concentration gradient affects the saturation rate and breakthrough time, or in other words, the diffusion process is concentration dependent for each dye. As seen in Figs. 5–7, for the three dyes the larger the influent concentration the steeper is the slope of breakthrough curve and smaller is the breakthrough time. The increase in adsorption capacity as the influent concentration increased can be explained by the fact that more adsorption sites were being covered as the dye ions concentration increased.

Breakthrough curves obtained at different dye levels show that among the three dye compounds studied the Gemacion Red H-E7B(A) dye was better adsorbed than Gemazol Turquise Blue-G and Gemactive Black HFGR dyes in all cases as the breakthrough time for Gemacion Red H-E7B(A) is greater than other dyes. In the case of the red dye, for a 751.3 mg l^{-1} inlet dye concentration of this adsorbate, biomass was capable of retaining 1007.8 mg dye per gram of sorbent.

4.3. Estimation of breakthrough curves and determination of kinetic constants

The column data obtained for each dye were fitted to the Thomas model to determine the Thomas rate constant (k_{Th}) and maximum solid-phase concentration (q_{0Th}). Respective values of k_{Th} and q_{0Th} calculated from the $\ln((C_0/C) - 1)$ versus V_{eff} plots at all flow rates and inlet dye concentrations studied are presented in Table 3 along with the correlation coefficients. Inspection of each of the regressed lines indicated that they were all acceptable fits with linear regression coefficients ranging from 0.963 to 0.997. The value of kinetic constant was influenced by both flow rate and dye concentration. In general the value of k_{Th} increased with increasing flow rate indicating the overall system kinetics was dominated by external mass transfer and decreased with increasing inlet dye concentration. As expected the bed capacity q_{0Th} reduced with increasing flow rate and increased with increasing inlet dye concentration for each dye studied. The dynamic behavior of the column predicted with the Thomas model are shown in Figs. 1–3 and 5–7 with the superposition of experimental results (symbols) and the theoretical calculated points (lines) for each dye. It appears that the simulation of the whole breakthrough for all flow rates and inlet concentrations studied is effective with the Thomas model and the breakthrough curves computed from this model is in good agreement with experimental data for all the dyes studied. This model is one of the most general and widely used theoretical methods to describe column performance. The suitability of Thomas model may be explained that the model assumes the external and internal diffusions are not the limiting step, Langmuir kinetics of adsorption–desorption is valid and no axial dispersion is derived with the adsorption. However adsorption is usually not limited by chemical reaction kinetics but is often controlled by interphase mass transfer and the effect of axial dispersion may be important especially at lower flow rates [23,28,31]. This discrepancy can lead some error when

this method is used to model adsorption process as seen in these sorbate–sorbent systems.

A simple theoretical model developed by Yoon and Nelson was also applied to investigate the breakthrough behavior of Gemacion Red H-E7B(A), Gemazol Turquise Blue-G and Gemactive Black HFGR dyes on dried *R. arrhizus* column. A linear regression was then performed on each set of transformed data to determine the coefficients from slope and intercept. The values of parameters k_{YN} (rate constant) and τ (the time required for 50% adsorbate breakthrough) in this model were determined at three different flow rate and four concentration levels for each dye. These values were used to calculate the entire breakthrough curves. It was found that the calculated theoretical breakthrough curves are in high agreement with the corresponding experimental data (Figs. 1–3 and 5–7). The values of k_{YN} and τ are presented in Table 3. As both the flow rate and inlet dye concentration increased, the values of k_{TH} increased and the values of τ decreased. The time required for 50% sorbate breakthrough (τ) obtained from the Yoon and Nelson model agreed well with the experimental data at all conditions examined. In general, good fits were obtained in all cases with correlation coefficients ranging from 0.983 to 0.994. Since the column capacity cannot be obtained from the Yoon and Nelson model directly and major process variables such as flow rate, influent dye concentration and adsorbent quantity, which are essential to determine the column capacity, are not incorporated in the Yoon and Nelson model, Eq. (8). was developed as a function of τ in order to find the column sorption capacity with these variables under varying experimental conditions. The bed capacity values (q_{0YN}) calculated from Eq. (8) are also presented in Table 3. The bed capacity q_{0YN} decreased with increasing flow rate and increased with increasing inlet dye concentration similar to change of Thomas sorption capacity with these parameters. In general the Yoon and Nelson model is capable of modeling symmetric breakthrough curves and neglects the effect of axial dispersion, but some deviations between model simulations and experimental breakthrough curves were observed in this study in cases where the curves are of asymmetric shape [25,32].

The data in the Table 3 also indicated negligible or evident differences between the experimental and predicted values of the bed capacity for both models and for all dyes without regard to flow rate, inlet dye concentration and dye type. In general Thomas model overestimated the bed capacity while Yoon–Nelson model predicted the bed capacity somewhat lower than that of experimental column capacity. Nevertheless from the results, it can be said that both the models were able to describe the column data well with high correlation coefficients.

5. Conclusion

The biosorption of Gemacion Red H-E7B(A), Gemazol Turquise Blue-G and Gemactive Black HFGR reactive dyes from aqueous solutions on a packed bed of dried *R. arrhizus* was investigated in a continuous mode. It was found that the sorption of each dye is influenced by the flow rate as well as by the inlet dye concentration. As the flow rate increased, the breakthrough curve became steeper, the break point time and the amount of adsorbed dye decreased, probably due to an insufficient residence time of the dye solution in the column. The breakthrough capacity of the sorbent was found to increase with inlet dye concentration and was in agreement with the finding of published literature. The Thomas and Yoon–Nelson models were applied to experimental data to predict the breakthrough curves and to determine the column capacity. It was seen that the full description of breakthrough could be accomplished by both the models at all flow rates and inlet dye concentrations studied for each dye while kinetic constants determined by linear regression techniques were proposed for the use in column design. Based on the q_0 values obtained, biosorption of dyes on biomass followed Gemacion Red H-E7B(A) > Gemazol Turquise Blue-G > Gemactive Black HFGR order with a capacity of 1007.8, 823.8, and 635.7 mg g^{-1} for GR, GTB, GB dyes at the highest inlet dye concentration of approximately 750 mg l^{-1} and at the minimum flow rate of 0.8 ml min^{-1}, respectively.

This study also identified the dried *R. arrhizus* as a suitable biosorbent – with good mechanical stability, flow permeability and higher dye uptake capacity – to be utilized for continuous removal of Gemacion Red H-E7B(A), Gemazol Turquise Blue-G and Gemactive Black HFGR reactive dyes from aqueous solution in a packed bed. The rapid adsorption and high uptake capacity for Gemacion Red H-E7B(A), Gemazol Turquise Blue-G and Gemactive Black HFGR reactive dyes make the fungus *R. arrhizus* with a promising future as an alternative to more costly materials such as activated carbon.

Acknowledgements

We thank Hacettepe University Research Fond Project No. 01.01.602.010, for partial financial support.

References

[1] E.A. Clarke, R. Anliker, Organic dyes and pigments, in: Handbook of Environmental Chemistry Anthropogenic Compounds, Springer, New York, 1980.
[2] H. Zollinger, Color Chemistry—Synthesis Properties and Applications of Organic Dyes and Pigments, VCH, New York, 1987.
[3] Y.M. Slokar, A.M. Le Marechal, Methods of decoloration of textile wastewaters, Dyes Pigments 37 (1997) 335–356.
[4] G. Crini, Non-conventional low-cost adsorbents for dye removal: a review, Biores. Technol. 97 (2006) 1061–1085.
[5] T. Robinson, G. McMullan, R. Marchant, P. Nigam, Remediation of dyes in textile effluent: a critical review on current treatment technologies with a proposed alternative, Biores. Technol. 77 (2001) 247–255.
[6] E. Forgacs, T. Cserhati, G. Oros, Removal of synthetic dyes from wastewaters: a review, Environ. Int. 30 (2004) 953–971.
[7] Y. Fu, T. Viraraghavan, Fungal decolorization of wastewaters: a review, Biores. Technol. 79 (2001) 251–262.
[8] Z. Aksu, Application of biosorption for the removal of organic pollutants: a review, Process Biochem. 40 (2005) 997–1026.
[9] M. Tsezos, J.P. Bell, Comparison of the biosorption and desorption of hazardous organic pollutants by live and dead biomass, Water Res. 23 (1989) 563–568.
[10] C.J. Banks, M.E. Parkinson, The mechanism and application of fungal biosorption to color removal from raw water, J. Chem. Technol. Biotechnol. 54 (1992) 192–196.

[11] T.-L. Hu, Removal of reactive dyes from aqueous solution by different bacterial genera, Water Sci. Technol. 34 (1996) 89–95.
[12] Z. Aksu, S. Tezer, Equilibrium and kinetic modelling of biosorption of Remazol Black B by *R. arrhizus* in a batch system: effect of temperature, Process Biochem. 36 (2000) 431–439.
[13] S. Sumathi, B.S. Manju, Uptake of reactive textile dyes by *Aspergillus foetidus*, Enzyme Microb. Technol. 27 (2000) 347–355.
[14] H.C. Chu, K.M. Chen, Reuse of activated sludge biomass. I. Removal of basic dyes from wastewater biomass, Process Biochem. 37 (2002) 595–600.
[15] T. O'Mahony, E. Guibal, J.M. Tobin, Reactive dye biosorption by *Rhizopus arrhizus* biomass, Enzyme Microb. Technol. 31 (2002) 456–463.
[16] Z. Aksu, G. Dönmez, A comparative study on the biosorption characteristics of some yeasts for Remazol Blue reactive dye, Chemosphere 50 (2003) 1075–1083.
[17] Z. Aksu, S. Tezer, Biosorption of reactive dyes on the green alga *Chlorella vulgaris*, Process Biochem. 40 (2005) 1347–1361.
[18] F. Kargi, S. Ozmihci, Comparison of adsorption performances of powdered activated sludge and powdered activated carbon for removal of turquoise blue dyestuff, Process Biochem. 40 (2005) 2539–2544.
[19] E. Valdman, L. Erijman, F.L.P. Pessoa, S.G.F. Leite, Continuous biosorption of Cu and Zn by immobilized waste biomass *Sargassum* sp, Process Biochem. 36 (2001) 869–873.
[20] Z. Zulfadhly, M.D. Mashitah, S. Bhatia, Heavy metals removal in fixed-bed column by the macro fungus *Pycnoporus sanguineus*, Environ. Pollut. 112 (2001) 463–470.
[21] T. Robinson, B. Chandran, G.-S. Naidu, P. Nigam, Studies on the removal of dyes from a synthetic textile effluent using barley husk in static-bath and in a continuous flow packed-bed reactor, Biores. Technol. 85 (2002) 43–49.
[22] F. Rozada, L.F. Calvo, A.I. GarcÌa, J. MartÌn-Villacorta, M. Otero, Dye adsorption by sewage sludge-based activated carbons in batch and fixed-bed systems, Biores. Technol. 87 (2003) 221–230.
[23] Y.F. u, T. Viraraghavan, Column studies for biosorption of dyes from aqueous solutions on immobilised *Aspergillus niger* fungal biomass, Water SA 29 (2003) 465–472.
[24] S. Netpradit, P. Thiravetyan, S. Towprayoon, Evaluation of metal hydroxide sludge for reactive dye adsorption in a fixed-bed column system, Water Res. 38 (2004) 71–78.
[25] S.-H. Lin, R.-S. Juang, Y.-H. Wang, Adsorption of acid dye from water onto pristine and acid-activated clays in fixed beds, J. Hazard. Mater. 113 (2004) 195–200.
[26] B.-Y. Chen, S.-Y. Chen, J.-S. Chan, Immobilized cell fixed-bed bioreactor for wastewater decolorization, Process Biochem. 40 (2005) 3434–3440.
[27] N. Ozturk, D. Kaval, Adsorption of boron from aqueous solutions using fly ash: batch and column studies, J. Hazard. Mater. 127 (2005) 81–88.
[28] Z. Aksu, F. Fien Çagatay, Investigation of biosorption of Gemazol Turquise Blue-G reactive dye by dried *Rhizopus arrhizus* in batch and continuous systems, Sep. Purif. Technol. 48 (2006) 24–35.
[29] T.V.N. Padmesh, K. Vijayaraghavan, G. Sekaran, M. Vela, Biosorption of Acid Blue 15 using fresh water macroalga *Azolla filiculoides*: batch and column studies, Dyes Pigments 71 (2006) 77–82.
[30] K.H. Chu, Improved fixed bed models for metal biosorption, Chem. Eng. J. 97 (2004) 233–239.
[31] H.C. Thomas, Heterogeneous ion exchange in a flowing system, J. Am. Chem. Soc. 66 (1944) 1664–1666.
[32] Y.H. Yoon, J.H. Nelson, Application of gas adsorption kinetics. I. A theoretical model for respirator cartridge service time, Am. Ind. Hyg. Assoc. J. 45 (1984) 509–516.